

Revisiting the Floquet-Bloch theory for an exactly solvable model of one-dimensional crystals in strong laser fields

Tatsuhiko N. Ikeda

Institute for Solid State Physics, University of Tokyo, Kashiwa, Chiba 277-8581, Japan

(Dated: May 21, 2018)

We revisit the Floquet-Bloch eigenstates of a one-dimensional electron gas in the presence of the periodic Kronig-Penney potential and an oscillating electric field. Considering the appropriate boundary conditions for the wave function and its derivative, we derive the determining equations for the Floquet-Bloch eigenstates, which are represented by a single-infinite matrix rather than a double-infinite matrix needed for a generic potential. We numerically solve these equations, showing that there appear anticrossings at the crossing points of the different Floquet bands as well as the band gaps at the edges and the center of the Brillouin zone. We also calculate the high-harmonic components of the electric current carried by the Floquet-Bloch eigenstates, showing that the harmonic spectrum shows a plateau for a strong electric field.

I. INTRODUCTION

High-harmonic generation (HHG) in bulk crystals has recently attracted much attention owing to its successful observation in the strong laser field [1–6]. HHG in solids in the nonperturbative regime thus achieved has shown different characters from that in atomic gases [7, 8], such as the multiple plateaus [5] and the linear scaling of the high-energy cutoff with the electric field rather than the laser intensity [1, 2, 4]. Although the microscopic mechanism of HHG in solids is still under an active debate [9–12], it is pointed out that the interband transitions between multiple bands play an essential role [5, 13–19].

The most fundamental model to discuss HHG in solids is a one-dimensional electron gas in the presence of both a periodic lattice potential and an oscillating electric field. Recently, this model has been shown to reproduce some aspects of experimental results by numerical simulations, in which the time-dependent Schrödinger equation is explicitly solved at each time step [16, 17, 19–21]. A complementary approach to this problem is the Floquet-Bloch theory [22–28], which utilizes the periodicity both in time and space to obtain the eigenstates for the time-dependent Schrödinger equation. In this approach, one needs to treat a double-infinite Hamiltonian matrix, where its column or row is labeled by two integers corresponding to the high harmonics for the time and space oscillation of the wave function. Although approximate solutions are obtained numerically [22], the numerical cost grows rapidly to achieve high accuracy.

The Kronig-Penney, or a square wave, potential [29] simplifies the problem significantly. This potential has traditionally deepened our understanding of the band gaps in solids because it is analytically solvable in the limit of each square approaching a delta function (see Eq. (3)). The analytical approach to the Floquet-Bloch theory for this potential was discussed by Faisal and Geeneser [23, 24], who proposed that the problem of the double-infinite Hamiltonian matrix can be reduced to that of a single-infinite matrix and the calculation cost is

thereby greatly decreased. However, their result contains mistakes stemming from their misunderstanding that the Floquet Green function is obtained by a simple generalization of the time-independent problem. Also, the high-harmonic components of the electric current have not been obtained in the delta-function limit.

In this paper, we revisit the Floquet-Bloch theory for the one-dimensional electron gas with the Kronig-Penney potential in the delta-function limit and analytically derive the correct determining equation for the Floquet-Bloch eigenstates. As suggested in Refs. [23, 24], this equation consists of a single-infinite matrix rather than a double-infinite one. We then numerically solve the equation, obtaining the quasienergy dispersion. In addition to the energy gaps at the edges and the center of the Brillouin zone that are already present in the oscillating electric field, there appear anticrossings between different Floquet bands owing to the interplay of the periodic potential and the oscillating electric field. We then calculate the high-harmonic components of the electric current carried by the Floquet-Bloch eigenstates that are obtained in this formalism. We show that, for a strong laser field, the high-harmonic components do not decay exponentially, but show a plateau.

The rest of this paper is organized as follows. In Sec. II, we formulate the problem that is addressed in this paper. By invoking the Floquet theorem, we derive an eigenvalue problem for a Floquet Hamiltonian. In Sec. III, we invoke the Bloch theorem and derive the determining equation for the quasienergy dispersion from the conditions for the connections of the wave function and its derivative. In Sec. IV, we solve the equation to obtain the quasienergy dispersion and discuss the band gaps and the anticrossings between the Floquet bands. We then calculate the high-harmonic components of the electric current for the Floquet-Bloch eigenstates thus obtained. The conclusions of this paper are summarized and some future perspectives are shown in Sec. V. In Appendix, we point out why the original derivation [23, 24] is not correct while it works in the absence of the oscillating

electric field.

II. FORMULATION OF THE PROBLEM

Let us begin by considering the following Hamiltonian in the velocity gauge

$$\mathcal{H}(t) = \frac{1}{2} [-i\partial_x - eA(t)]^2 + V(x). \quad (1)$$

Here e (< 0) denotes the charge of an electron, and we work in the units of $\hbar = m = 1$ and use the abbreviation $\partial_x = \partial/\partial x$ throughout this paper. The vector potential

$$A(t) = A_0 \cos(\Omega t) \quad (2)$$

represents the uniform laser electric field along the x axis, and the periodic lattice potential $V(x)$ is taken to be the Kronig-Penney one in the delta-function limit:

$$V(x) = \frac{P}{2a} \sum_{p=-\infty}^{\infty} \delta(x - pa), \quad (3)$$

where a and P denote the lattice constant and the strength of the lattice potential, respectively. We note that $A(t)$ and $V(x)$ are both periodic: $A(t + T) = A(t)$ and $V(x + a) = V(x)$ with $T \equiv 2\pi/\Omega$.

Our aim is to solve the time-dependent Schrödinger equation for the Hamiltonian (1) which is equivalent to find the eigenstates with the zero eigenvalue for the operator

$$\mathcal{K}_0(t) = i\partial_t - \mathcal{H}(t). \quad (4)$$

To this end, we eliminate the term proportional to $A(t)^2$ from $\mathcal{H}(t)$ by making the phase transformation

$$\mathcal{K}(t) = e^{i\theta(t)} \mathcal{K}_0(t) e^{-i\theta(t)} = i\partial_t - H(t), \quad (5)$$

$$H(t) = -\frac{1}{2} \partial_x^2 + ieA(t)\partial_x + V(x), \quad (6)$$

where $\theta(t) \equiv \exp(-\frac{i}{2} \int_0^t A(s)^2 ds)$ and $\partial_t = \partial/\partial t$. We note that the operator $\mathcal{K}(t)$ has discrete translation symmetries in the t and x directions due to the periodicities of $A(t)$ and $V(x)$, respectively.

The discrete translation symmetry in time simplifies the problem of finding zero modes of $\mathcal{K}(t)$. This symmetry tells us that an eigenstate $\Psi(x, t)$ of $\mathcal{K}(t)$ is written as $\Psi(x, t) = e^{-iEt} \Psi_E(x, t)$, where $\Psi_E(x, t)$ is a periodic function $\Psi_E(x, t + T) = \Psi_E(x, t)$. We refer to E as the quasienergy since E can be taken in a certain region such as $[0, \Omega]$. However, we do not restrict E on such a region in this paper, but work in the extended zone scheme, in which we have physically equivalent states that have equal E modulo Ω . Expanding $\Psi_E(x, t)$ in the Fourier series, we obtain the following expression for an eigenstate

$$\Psi(x, t) = e^{-iEt} \sum_{n \in \mathbb{Z}} \psi_n(x) e^{in\Omega t}. \quad (7)$$

Now the equation $\mathcal{K}(t)\Psi(x, t) = 0$, which we aim to solve, reduces to the following form:

$$\sum_n H_{mn}^0 \psi_n(x) + V(x) \psi_m(x) = E \psi_m(x), \quad (8)$$

$$H_{mn}^0 = \left(-\frac{1}{2} \partial_x^2 + n\Omega \right) \delta_{mn} + i\Omega \frac{\alpha_0}{2} (\delta_{m,n+1} + \delta_{m,n-1}) \partial_x, \quad (9)$$

where $\alpha_0 \equiv eA_0/\Omega$ represents the coupling strength between the electron and the oscillating electric field.

The discrete translation symmetry in space also simplifies the problem, but this is not enough for the complete solution in general. A parallel argument on space reduces the continuous variable x to an integer and the remaining problem is to diagonalize a double-infinite matrix where its row or column is characterized by a pair of integers corresponding to the high harmonics for the time and space oscillation of the wave function. Although we can numerically obtain approximate solutions for the problem, the computational complexity grows rapidly in increasing the precision.

III. SOLUTION TO THE EIGENVALUE PROBLEM

The Kronig-Penney potential (3) enables us to proceed further analytically. In this section, we analyze the eigenvalue problem (8) and (9) in the real space, and show that the quasienergy E is obtained as a root of a secular equation for a single-infinite matrix (see Eq. (23) or (26) below).

Before solving our problem, we consider the solution in the absence of the periodic potential:

$$H^0 \psi(x) = E \psi(x). \quad (10)$$

In this case, the normalizable eigenstate characterized by a real momentum k and an integer N is given by

$$\varphi_n^{N,k}(x) = J_{n-N}(\alpha_0 k) e^{ikx} \quad (11)$$

and its eigenvalue of H^0 is

$$\epsilon_0^N(k) = \frac{k^2}{2} + N\Omega. \quad (12)$$

Here $J_n(x)$ denotes the Bessel function of the first kind. One can easily confirm that Eq. (11) satisfies Eq. (10) by acting H^0 onto $\varphi_n^{N,k}(x)$ and using the identity $J_{n+1}(x) + J_{n-1}(x) = 2nJ_n(x)/x$ [30]. We note that the eigenstates (11) are mutually orthogonal and satisfy the completeness relation

$$\sum_{N \in \mathbb{Z}} \int_{-\infty}^{\infty} \frac{dk}{2\pi} \varphi_n^{N,k}(x) \varphi_{n'}^{N,k}(x')^* = \delta_{nn'} \delta(x - x'). \quad (13)$$

This can be proved by using Neumann's identities [30]

$$\sum_{m \in \mathbb{Z}} J_{n \pm m}(z) J_m(w) = J_n(z \mp w) \quad (14)$$

and $J_{n-m}(0) = \delta_{nm}$.

We treat the effects of the periodic potential $V(x)$ as appropriate boundary conditions for the unit cell. the Bloch theorem tells us that an eigenstate $\psi(x)$ satisfies

$$\psi(a) = e^{iK_a} \psi(0) \quad (15)$$

for a lattice momentum K with $-\pi/a \leq K < \pi/a$. In addition, the Kronig-Penney potential (3) imposes boundary conditions for the first derivatives. By integrating both sides of Eq. (8) over $x \in [-\epsilon, \epsilon]$ and taking the limit of $\epsilon \downarrow 0$, we obtain

$$\partial_x \psi(0+) - e^{-iK_a} \partial_x \psi(a-) - \frac{P}{a} \psi(0) = 0, \quad (16)$$

where we have used $\partial_x \psi(0-) = e^{-iK_a} \partial_x \psi(a-)$ which the Bloch theorem implies. Since $V(x)$ vanishes on $0 < x < a$, our problem is to solve

$$H^0 \psi(x) = E(K) \psi(x) \quad (0 < x < a) \quad (17)$$

with the boundary conditions (15) and (16). The notation $E(K)$ emphasizes the fact that the quasienergy bands over the first Brillouin zone are obtained by varying K appearing in the boundary conditions (15) and (16).

The most general solution of Eq. (17) is of the form

$$\psi_n(x) = \sum_{N \in \mathbb{Z}} [A_N \varphi_n^{N, k_N}(x) + B_N \varphi_n^{N, -k_N}(x)], \quad (18)$$

with

$$k_N \equiv \sqrt{2[E(K) - N\Omega]}. \quad (19)$$

We note that there is no problem if k_N becomes imaginary since we do not now work on $-\infty < x < \infty$, but a finite range $0 < x < a$.

The coefficients $\{A_N\}_N$ and $\{B_N\}_N$ are determined by the boundary conditions (15) and (16). By substituting the general solution (18) into these conditions, we obtain the following homogeneous matrix equation

$$\sum_{N \in \mathbb{Z}} \begin{pmatrix} \mathcal{M}_{nN}^{11} & \mathcal{M}_{nN}^{12} \\ \mathcal{M}_{nN}^{21} & \mathcal{M}_{nN}^{22} \end{pmatrix} \begin{pmatrix} A_N \\ B_N \end{pmatrix} = 0, \quad (20)$$

where the infinite matrix \mathcal{M}_{nN}^{ij} in a 2×2 block form is defined as

$$\begin{pmatrix} \mathcal{M}_{nN}^{11} & \mathcal{M}_{nN}^{12} \\ \mathcal{M}_{nN}^{21} & \mathcal{M}_{nN}^{22} \end{pmatrix} = C_N \begin{pmatrix} J_{n-N}(\alpha_0 k_N) & 0 \\ 0 & J_{n-N}(-\alpha_0 k_N) \end{pmatrix} \quad (21)$$

with

$$C_N = \begin{pmatrix} e^{ik_N a} - e^{iK a} & e^{-ik_N a} - e^{iK a} \\ ik_N(1 - e^{i(k_N - K)a}) - \frac{P}{a} & -ik_N(1 - e^{i(-k_N - K)a}) - \frac{P}{a} \end{pmatrix} \quad (22)$$

Equation (24) has a nontrivial solution when $E(K)$ is chosen so that

$$\det \mathcal{M} = 0, \quad (23)$$

and the coefficients $\{A_N\}_N$ and $\{B_N\}_N$ are determined up to the overall factor. We note that, if $E(K) = M\Omega$ for an integer M and thus $k_M = 0$, the $N = M$ components are considered to be eliminated from the matrix since $\varphi_n^{M,0}$ cannot satisfy the boundary conditions for $P \neq 0$.

When solved for $E(K)$ for each K , the secular equation (23) gives the quasienergy dispersions in the presence of the oscillating electric field. The multiple solutions obtained for a given K correspond to the different bands. We note that the row and the column of \mathcal{M} are labeled by the pair of (n, i) and $(N, i) \in \mathbb{Z} \times \{1, 2\}$, which have been remarkably simplified. As noted in the previous section, if we had not used the explicit form of the Kronig-Penney potential (3) but had only invoked the periodicity in space, we would have obtained a matrix whose column or row runs over $\mathbb{Z} \times \mathbb{Z}$ corresponding to the high harmonics for the wave function oscillations in time and space.

Another representation for the secular equation (23) is obtained, where the column and the row of the matrix is treated on equal footing. We multiply both sides of Eq. (24) by $J_{n-N'}(\alpha_0 |k_{N'}|)$ and sum them over n , obtaining

$$\sum_{N \in \mathbb{Z}} \begin{pmatrix} \mathcal{W}_{N'N}^{11} & \mathcal{W}_{N'N}^{12} \\ \mathcal{W}_{N'N}^{21} & \mathcal{W}_{N'N}^{22} \end{pmatrix} \begin{pmatrix} A_N \\ B_N \end{pmatrix} = 0, \quad (24)$$

where the matrix elements of $\mathcal{W}_{N'N}$ are defined by

$$\begin{pmatrix} \mathcal{W}_{N'N}^{11} & \mathcal{W}_{N'N}^{12} \\ \mathcal{W}_{N'N}^{21} & \mathcal{W}_{N'N}^{22} \end{pmatrix} = C_N \begin{pmatrix} J_{N'N}^{(-)} & 0 \\ 0 & J_{N'N}^{(+)} \end{pmatrix} \quad (25)$$

with $J_{N'N}^{(\pm)} \equiv J_{N-N'}(\alpha_0(|k_{N'}| \pm k_N))$. Making use of $|k_{N'}|$ in the procedure is technically advantageous since it ensures that $\det \mathcal{W}$ is real or pure imaginary for any value of $E(K)$. We assume that the matrix $J_{n-N}(\alpha_0 |k_N|)$ has a nonzero determinant when n and N are regarded as the labels for its row and column, respectively. Then the secular equation (23) is equivalent to

$$\det \mathcal{W} = 0. \quad (26)$$

In the absence of the electric field, the secular equations (23) and (26) reproduce the well-known Kronig-Penney dispersion relation [29]

$$\cos K a = \cos k_0 a + \frac{P}{2k_0 a} \sin k_0 a \quad (27)$$

with $k_0 = \sqrt{2E(K)}$. To confirm this, let us note that the absence of the electric field implies that N only takes 0 and the Bessel functions $J_{n-N}(\pm\alpha_0)$ and $J_{NN'}^{(\pm)}$ are replaced by unity. Then the secular equations read $\det C_0 = 0$, which readily leads to Eq. (27).

IV. PROPERTIES OF THE FLOQUET-BLOCH EIGENSTATES

In this section, we numerically solve the equations derived in the previous section and discuss the properties of the Floquet-Bloch eigenstates. For simplicity, we set the lattice constant a as unity throughout this section.

A. Absence of the periodic potential

Before discussing the effects of the periodic potential, we investigate the properties of the Floquet eigenstates (11) in the absence of the periodic potential.

The quasienergy of $\varphi^{N,k}$ is given by Eq. (12), which is illustrated in Fig. 1 (a). The horizontal axis of Fig. 1 (a) shows k modulo 2π for the comparison below to $E(K)$ in the presence of the periodic potential. The quasienergy with $N = 0$ is identical to $k^2/2$ in spite of the coupling to the oscillating electric field. In addition to the dispersion relation $k^2/2$ for $N = 0$, we have an infinite number of replicas with equal spacings Ω since we work in the extended zone scheme as noted above. In the following, we refer to the set of (quasi)energy for a given N as the Floquet band.

Now we define the high-harmonic distribution:

$$w_n^N(k) \equiv |\varphi_n^{N,k}(x)|^2 = J_{n-N}(\alpha_0 k)^2. \quad (28)$$

This represents the weight of the Floquet eigenstate $\varphi_n^{N,k}(x)$ on the oscillating component with frequency $\epsilon_0^N(k) - n\Omega$ (see Eq. (7)). We note that $w_n(k)$ is normalized as

$$\sum_{n \in \mathbb{Z}} w_n^N(k) = 1, \quad (29)$$

which follows from Eq. (14). Since $w_{n+1}^{N+1}(k) = w_{n-1}^N(k)$ holds true, it is enough to discuss $w_n^0(k)$. In addition, we have $w_{-n}^0(k) = w_n^0(-k) = w_n^0(k)$, and, hence, the nontrivial information is contained in $w_n^0(k)$ for, say, $n \geq 0$ and $k \geq 0$. In contrast to the quasienergy, the high-harmonic distribution depends on the coupling strength α_0 between the electron and the electric field.

The high-harmonic distribution $w_n^0(k)$ is illustrated in Fig. 1 (b) for several values of k . First, we note $w_n^0(k=0) = \delta_{n0}$, which follows from the definition (28). This is because the electric field couples to the electron

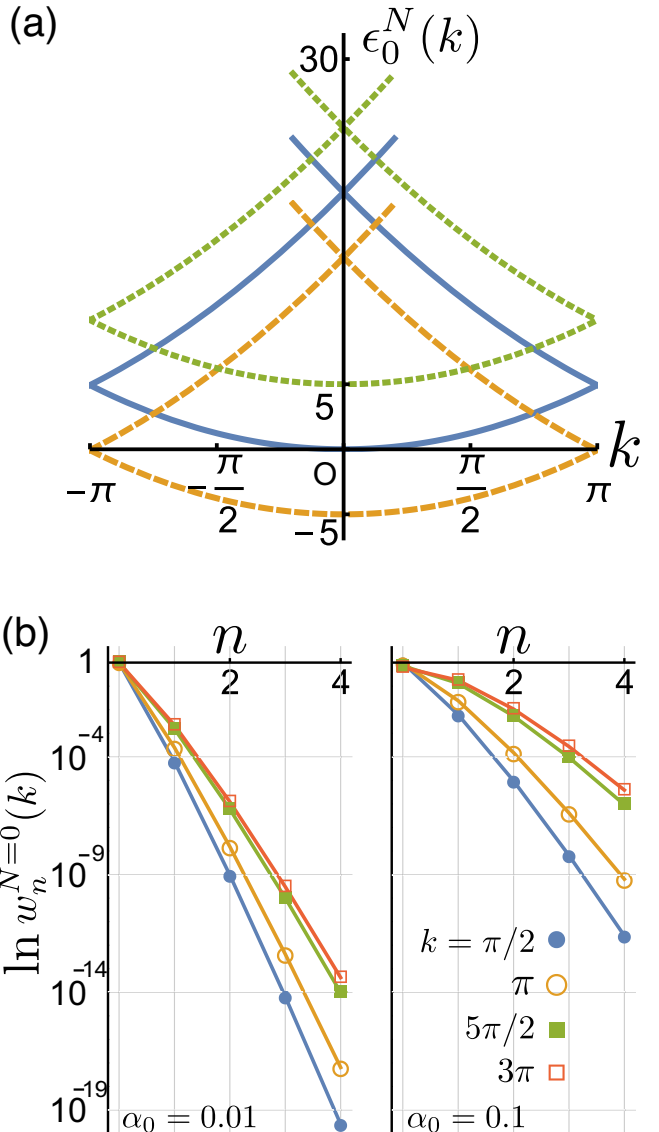


FIG. 1. (Color Online) (a) The quasienergy $\epsilon_0^N(k)$ [Eq. (12)] for $N = 0$ (solid), -1 (dashed), and 1 (dotted), in the absence of the periodic potential, $P = 0$, and $\Omega = 5$. The horizontal axis represents the momentum k modulo 2π . (b) The high-harmonic distribution $w_n^0(k)$ [Eq. (28)] for $\alpha_0 = 0.01$ (left) and 0.1 (right). Each dataset corresponds to the momentum $k = \pi/2$ (filled circle), π (open circle), $5\pi/2$ (filled square), and 3π (open square).

through its momentum and, thus, high-harmonic oscillation is not induced for the $k = 0$ state. Second, as k increases with α_0 held fixed or α_0 does with k held fixed, the width of the high-harmonic distribution $w_n^0(k)$ becomes larger. This tendency is qualitatively consistent with the fact the the coupling to the electric field is proportional to the momentum. We will show below in Sec. IV C that the width of $w_n^0(k)$ is related to the high-harmonic components of the electric current in the

presence of the periodic potential. We note that, as anticipated from the Bessel function in Eq. (28), $w_n^0(k)$ does not show a monotonous but an oscillatory behavior for even larger values of α_0 or k .

B. Effects of the periodic potential

The Floquet-band theorem [23] holds true also in the presence of the periodic potential. Namely, if $E(K)$ satisfies Eq. (26), then $E(K) + M\Omega$ does as well for any integer M . To prove this, let us suppose that Eq. (26) is satisfied for $E(K)$ and ask if $\det \tilde{\mathcal{W}} = 0$, where $\tilde{\mathcal{M}}$ is defined by replacing k_N in \mathcal{W} by $\tilde{k}_N = \sqrt{2[E(K) + M\Omega - N\Omega]} = k_{N-M}$. In this replacement, $J_{NN'}^{(\pm)}$ in \mathcal{W} is replaced by $\tilde{J}_{NN'}^{(\pm)} = J_{N'-N}(\alpha_0(|\tilde{k}_N| \pm \tilde{k}_{N'})) = J_{(N'-M)-(N-M)}(\alpha_0(|k_{N-M}| - k_{N'-M})) = J_{N-M, N'-M}^{(\pm)}$. Thus $\tilde{\mathcal{W}}$ is obtained by shifting the labels of both the row and the column of \mathcal{W} by M . Since this shift does not change the value of the determinant, we have obtained $\det \tilde{\mathcal{W}} = 0$.

Both in absence and presence of the coupling between the electron and the electric field, the quasienergy dispersion $E(K)$ is symmetric about $K = 0$. To prove this, let us suppose that Eq. (23) is satisfied for $E(K)$ and show that $E(K)$ also satisfies Eq. (23) with K replaced by $-K$. For this purpose, we try to transform the matrix \mathcal{M} for K into that for $-K$ by means of elementary row and column operations. The concrete procedure is the following. First we multiply every row in the upper (lower) blocks by $e^{-iK\alpha}$ ($e^{iK\alpha}$) and the N -th column in the left (right) blocks by $e^{-ik_N\alpha}$ ($e^{ik_N\alpha}$). Second we add the n -th row of the upper left (right) block of the resulting matrix multiplied by $-e^{-iK\alpha}P/a$ ($-e^{iK\alpha}P/a$) to the n -th rows of the lower left (right) blocks. Third we interchange the N -th columns of the left and right blocks for each N . In these three steps, the determinant is invariant or changes its sign depending on whether N is thought to be even or odd. The matrix thus obtained differs from \mathcal{M} for $-K$ only in that $J_{n-N}(\pm\alpha_0 k_N)$ appears in the opposite way in the form of Eq. (21). This difference does not matter when their determinants are compared, for $J_{n-N}(\pm\alpha_0 k_N) = (-1)^{n-N} J_{n-N}(\mp\alpha_0 k_N)$. Thus we have shown that, $E(K)$ satisfies $\det \mathcal{M} = 0$ for K , it also does for $-K$.

In the absence of the coupling between the electron and the electric field, or $\alpha_0 = 0$, the quasienergy dispersion obtained from Eq. (27) is shown in Fig. 2 (a). Here we also plot the Floquet bands for $N = \pm 1$ in addition to the original band $N = 0$. We note again that these states represent the same states as $N = 0$ since we work in the extended zone scheme in the energy direction. Comparing with Fig. 1 (a), we notice that the periodic potential gives rise to the energy gaps opening at $K = 0, \pm\pi$ where two energy bands touch each other in the absence

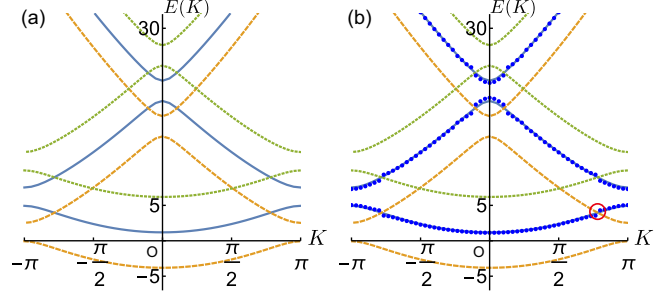


FIG. 2. (Color Online) (a) Quasienergy dispersion $E(K)$ for the lattice potential strength $P = 3$ in the absence of the coupling between the electric field and the electron, $\alpha_0 = 0$. Each line belongs to the Floquet band with $N = 0$ (solid), -1 (dashed), and 1 (dotted), and $\Omega = 5$. (b) Quasienergy dispersion $E(K)$ for $P = 3$, $\alpha_0 = 0.1$, and $\Omega = 5$ (filled circle). Only the quasienergies corresponding to $N = 0$ are plotted.

of the periodic potential.

The coupling between the electron and the electric field together with the periodic potential gives rise to the anticrossings of the quasienergy dispersion at the crossing points of the different Floquet bands. Figure 2 (b) shows the quasienergy $E(K)$ for $N = 0$, $\alpha_0 = 0.1$, $\Omega = 5$, and $P = 3$ obtained from Eq. (26) with the restriction of $N = 0, \pm 1, \dots, \pm 5$. The quasienergy $E(K)$ is close to the one for $\alpha_0 = 0$ with $N = 0$ except for the vicinity of the crossing points with $N = \pm 1$. One can also find small jumps of the data at the crossing points between $N = 0$ and $N = \pm 2$, but cannot between $N = 0$ and $N = \pm 3, \dots, \pm 5$. This is because the coupling between the Floquet bands is proportional to $J_{N'N}^{(\pm)}$ (see Eq. (25)), which rapidly decreases as $|N' - N|$ increases.

The cutoff for N in solving Eq. (26) to obtain the $N = 0$ band is justified for a moderate value of α_0 . To confirm this, we investigate the quasienergy by solving Eq. (26) for $\Omega = 5$ and $P = 3$ with $N = 0, \pm 1, \pm 2, \dots, \pm N_{\text{cut}}$, where N_{cut} is a varying cutoff. Figure 3 shows the size of the anticrossing at the point indicated by a circle in Fig. 2(b) calculated for N_{cut} ranging from 1 to 10. For the smaller values of $\alpha_0 = 0.01$ and 0.1 , $N_{\text{cut}} = 2$ is large enough to achieve a 10^{-4} accuracy for the eigenenergy. For a larger value of $\alpha_0 = 0.3$, the quasienergies show oscillations up to 10% magnitude at $N_{\text{cut}} \leq 3$, and then converge at $N_{\text{cut}} = 5$ within an accuracy of 10^{-3} . We note that $\alpha_0 = 0.3$ roughly corresponds to $|A_0| = \pi/2$ in the unit of $|e| = 1$ since we set $\Omega = 5$ in our calculation.

We remark that it becomes more complicated to interpret each quasienergy for $\alpha_0 \gtrsim 0.3$ because the coupling to the higher Floquet bands are not negligible and

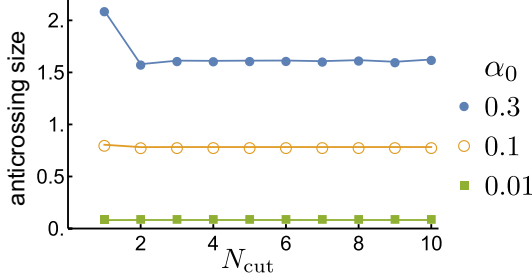


FIG. 3. (Color Online) Anticrossing size at the point indicated by a circle in Fig. 2(b) plotted against the cutoff N_{cut} ranging from 1 to 10 calculated for $P = 3$ and $\Omega = 5$. Each set of the data corresponds to the different coupling strength between the electron and the electric field: $\alpha_0 = 0.3$ (filled circle), 0.1 (open circle), and 0.01 (filled square).

more anticrossings appear at many K . In addition, some anticrossings become so large that it is not simple to keep track of the one-to-one correspondence between the quasienergy for $\alpha_0 \neq 0$ and 0. Of course, this is a matter of interpretation, and Eq. (26) still provides us with the quasienergy dispersion $E(K)$ even for such a large value of α_0 .

C. High-harmonic components of the electric current

Finally we discuss the electric current

$$j(x, t) = e \{ \text{Re}[\Psi^*(x, t)(-\text{i}\partial_x)\Psi(x, t)] - eA(t)|\Psi(x, t)|^2 \} \quad (30)$$

carried by the eigenstate $\Psi(x, t)$ [see Eq. (7)], which works as the source of HHG. We show below that the electric current involves high-harmonic components in the presence of the lattice potential.

In the absence of the lattice potential, the electric current (30) does not involve any high harmonics. This is because the momentum is a good quantum number and $-\text{i}\partial_x\Psi(x, t) = k\Psi(x, t)$ is satisfied for the eigenstate (11). From this relation, we obtain the electric current as $j(x, t) = e[k - eA(t)]$, which is homogeneous and contains only frequencies $\pm\Omega$.

In the presence of the lattice potential, the Floquet-Bloch eigenstate (18) consists of various momenta and high harmonics are involved in the current. To show this, we first compactify Eq. (18) as

$$\psi_n(x) = \sum_{N, \sigma=\pm} \mathcal{A}_N^\sigma \varphi_n^{N, \sigma k_N}(x), \quad (31)$$

where we have introduced the notations $\mathcal{A}_N^+ = A_N$ and $\mathcal{A}_N^- = B_N$. Together with Eq. (7), we obtain the nontrivial paramagnetic part of the electric current (30) averaged

over the unit cell as (we have been setting $a = 1$ in this section)

$$\mathcal{J}(t) \equiv e \int_0^1 dx \text{Re}[\Psi^*(x, t)(-\text{i}\partial_x)\Psi(x, t)] = \sum_n \mathcal{J}_n e^{in\Omega t} \quad (32)$$

with

$$\mathcal{J}_n \equiv e \sum_{\substack{N, N' \\ \sigma, \sigma', n}} \sigma k_N W_{\sigma' \sigma}^{N' N}(n) (\mathcal{A}_{N'}^{\sigma'})^* \mathcal{A}_N^\sigma, \quad (33)$$

where $W_{\sigma' \sigma}^{N' N}(n)$ represents the following wave-function overlap

$$W_{\sigma' \sigma}^{N' N}(n) \equiv \sum_m \int_0^1 dx \varphi_m^{N', \sigma' k_{N'}}(x)^* \varphi_{m+n}^{N, \sigma k_N}(x). \quad (34)$$

We note $\mathcal{J}_{-n} = \mathcal{J}_n^*$ since $\mathcal{J}(t)$ is real. Equation (32) shows that the current involves an oscillating component with frequency $n\Omega$ if $\mathcal{J}_n \neq 0$.

We make a brief remark on the symmetry of the high-harmonic current. First, the inversion symmetry of our problem relates the high-harmonic currents for the degenerate Floquet-Bloch eigenstates that belong to $\pm K$. If we introduce the notations $\mathcal{J}_n(\pm K)$ to distinguish these two, one can easily show

$$\mathcal{J}_n(-K) = (-1)^{n+1} \mathcal{J}_n(K). \quad (35)$$

Thus the high-harmonic currents for an even n vanish when summed over $\pm K$. Second, \mathcal{J}_n is real since our Hamiltonian (6) is symmetric under the product of the inversion and the time reversal.

The result (32) reduces to the case of no lattice potential if we put, for example, $A_N = \delta_{N,0}$ and $B_N = 0$, which correspond to the positive momentum state with momentum k_0 . In this case, one can easily see that $\mathcal{J}_n = +k_0 W_{++}^{00}(n) = k_0 \delta_{n0}$. Similarly, if we put $A_N = 0$ and $B_N = \delta_{N,0}$, which correspond to the negative momentum state with momentum $-k_0$, we obtain $p_n = -k_0 W_{--}^{00}(n) = -k_0 \delta_{n0}$. In both cases, the current does not involve any high harmonics as we have shown above.

The high harmonics are induced once neither A_N nor B_N vanishes as caused by the Kronig-Penney potential. To see this fact, we focus on the contributions to \mathcal{J}_n from $N = N'$ with real k_N , which consist of the diagonal ($\sigma = \sigma'$) and the off-diagonal ($\sigma \neq \sigma'$) parts. The diagonal parts are proportional to $|A_N|^2$ or $|B_N|^2$ and again do not contain high harmonics since they are proportional to δ_{n0} . On the other hand, the off-diagonal parts are proportional to $A_N^* B_N$ and $B_N^* A_N$ and involve a nontrivial dependence on n given by $J_n(2\alpha_0 k_N)$, which becomes nonzero for $n > 1$ in general.

We note that this type of high harmonics are closely related to the high-harmonic distribution (28). If the

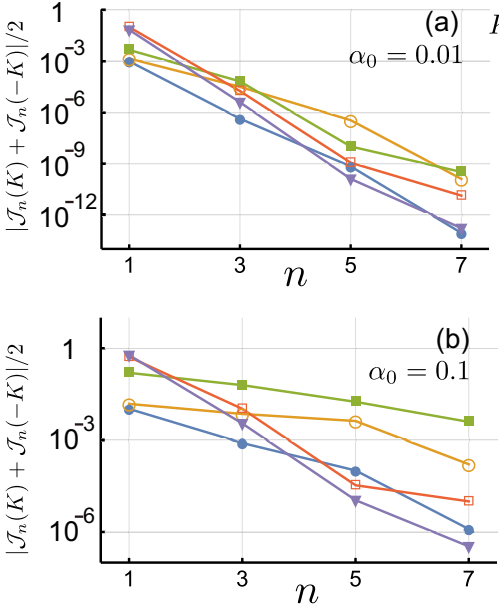


FIG. 4. (Color Online) K -resolved high-harmonic spectrum of the electric current, $|\mathcal{J}_n(K) + \mathcal{J}_n(-K)|/2$ in the unit of $|e|$, calculated for the Floquet-Bloch eigenstates corresponding to the lowest band in the absence of the oscillating electric field (the lowest data points in Fig. 2(b)). The two panels are the results for $\alpha_0 = 0.01$ (a) and 0.1 (b), and each data set corresponds to the lattice momentum $K = 0$ (filled circle), $\pi/4$ (open circle), $\pi/2$ (filled square), $3\pi/4$ (open square), and π (filled triangle).

high-harmonic distribution $|\varphi_n^{N,k}(x)|^2$ were trivially δ_{nN} , the wave-function overlap $W_{\sigma'\sigma}^{NN}(n)$ would vanish for any $n > 1$. Thus the width of the high-harmonic distribution roughly corresponds to the highest order of harmonics of the electric current.

Actually \mathcal{J}_n also contains the contributions from $N \neq N'$ and numerical calculations are needed to obtain the accurate values. Figure 4 shows the numerically calculated high-harmonic currents for the Floquet-Bloch eigenstates, which correspond to the lowest band in the absence of the oscillating electric field (see the lowest data points in Fig. 2 (b)). The wave function is renormalized so that $\int_0^1 dx |\Psi(x, 0)|^2 = 1$. Considering Eq. (35), we have focused on $|\mathcal{J}_n(K) + \mathcal{J}_n(-K)|/2$ to obtain the K -resolved information. As shown in Fig. 4, the high-harmonic current at every K decreases exponentially as n increases for a small coupling $\alpha_0 = 0.01$ between the electron and the oscillating electric field. On the other hand, for a larger coupling $\alpha_0 = 0.1$, the high-harmonic currents show plateau behaviors around $K = \pi/2$. Since these plateaus give the largest values for $n = 3, 5$, and 7, we also expect a plateau for $\mathcal{J}_n(K)$ summed over K ,

which is the source of HHG. Thus our result is qualitatively consistent with experiments.

V. CONCLUSIONS

We have revisited the Floquet-Bloch theory for a one-dimensional electron gas in the presence of the Kronig-Penney potential in the delta-function limit and the oscillating electric field. Taking advantage of the special form of the potential, we have shown that the Floquet-Bloch eigenstate is obtained from an eigenvalue problem for a single-infinite matrix, which is much simpler than the double-infinite matrix needed for generic periodic potentials. We have numerically solved the problem to obtain the quasienergy dispersion $E(K)$, and shown that it has the anticrossings at the crossing points of the Floquet bands as well as the band gaps at the edges and the center of the Brillouin zone. We have also confirmed that the quasienergy $E(K)$ is obtained at high precision especially for a small amplitude of the vector potential $|A_0| \lesssim \pi/2$ in the unit of $|e| = 1$. We have then calculated the high-harmonic components of the electric current for the Floquet-Bloch eigenstates thus obtained, showing that a plateau appears when the coupling between the electron and the oscillating electric field is strong enough.

Application to HHG in solids especially in the non-perturbative regime is of great interest. As shown by the time-dependent Schrödinger equation approach [19], the multiple-plateau structure of HHG is related to the characteristic amplitudes of the vector potential $|A_0| = \pi, 2\pi, 3\pi, \dots$ in the unit of $|e| = 1$. Once it is achieved to control our calculations at such a large amplitude, our approach will contribute to the better understand of HHG in solids. In addressing the strong coupling regime by the Floquet-Bloch theory, our single-infinite matrix formulation is expected to be of great benefit compared with the ordinary double-infinite matrix one.

ACKNOWLEDGEMENTS

Fruitful discussions with Hirokazu Tsunetsugu are gratefully acknowledged. This work was supported by JSPS KAKENHI Grant Nos. JP16H06718 and JP18K13495.

Appendix A: Floquet-Green function approach

In this appendix, we review the original approach to solve Eqs. (8) and (9) on the basis of the Floquet-Green functions by Faisal and Genieser [23, 24]. Unfortunately, their results contain mistakes, which we point out in the following.

The unperturbed Floquet-Green function $G_{nn'}^0(x, x')$ is defined by

$$(E - H^0)G_{nn'}^0(x, x') = \delta_{nn'}\delta(x - x') \quad (\text{A1})$$

and its explicit form is given by

$$G_{nn'}^0(x, x') = \sum_N \int_{-\infty}^{\infty} \frac{dk}{2\pi} \frac{\varphi_n^{Nk}(x)\varphi_{n'}^{Nk}(x')^*}{E - (k^2/2 + N\Omega) + i0}, \quad (\text{A2})$$

where $\varphi_n^{Nk}(x)$ is the eigenstate of H^0 (see Eq. (11)). In this appendix, the summation is taken over \mathbb{Z} if its range is not specified. The Floquet-Green function $G_{nn'}^0(x, x')$ enables us to transform Eq. (8) as

$$\psi_n(x) = \sum_{n'} \int_{-\infty}^{\infty} dx' G_{nn'}^0(x, x') V(x') \psi_{n'}(x'). \quad (\text{A3})$$

Once $G_{nn'}^0(x, x')$ is known, the quasienergy is obtained as follows. We invoke the Bloch theorem and assume that our eigenstate is written as

$$\psi_n(x) = e^{ikx} \phi_n^K(x), \quad (\text{A4})$$

where K is a lattice momentum and $\phi_n^K(x)$ is a periodic function: $\phi_n^K(x+a) = \phi_n^K(x)$. Similarly to the argument in Sec. III, this leads to the quasienergy E for each K , which is denoted as $E(K)$. By substituting Eqs. (3) and (A4) into Eq. (A3), we have

$$\phi_n^K(0) = \frac{P}{2a} \sum_{p, n'} G_{nn'}^0(0, pa) e^{ipK a} \phi_n^K(0), \quad (\text{A5})$$

where we have used the periodicity $\phi_n^K(pa) = \phi_n^K(0)$ for any $p \in \mathbb{Z}$. This is a linear homogeneous equation for $\phi_n^K(0)$ and the secular equation determines the quasienergy $E(K)$.

To obtain the simplified expression for $G_{nn'}^0(x, x')$, Faisal and Genieser [23, 24] performed the integration over k on the right-hand side of Eq. (A2) by invoking residue calculus. Focusing on the factor $e^{ik(x-x')}$ in the integrand, they added a contour integral along the

infinitely-large semicircle on the upper- or lower-half of the complex k plane depending on $x \geq x'$ or $x < x'$, respectively, assuming that this additional contour integral gives no contribution. Then they calculated the residues of the integrand at the poles encircled by the composite contour consisting of the real axis and the semicircle, obtaining, for $x \geq x'$,

$$G_{nn'}^{\text{FG}}(x, x') = -i \sum_N \frac{1}{k_N} J_{n-N}(\alpha_0 k_N) J_{n'-N}(\alpha_0 k_N) e^{ik_N(x-x')} \quad (\text{A6})$$

and, for $x < x'$,

$$G_{nn'}^{\text{FG}}(x, x') = -i \sum_N \frac{1}{k_N} J_{n-N}(-\alpha_0 k_N) J_{n'-N}(-\alpha_0 k_N) e^{-ik_N(x-x')}, \quad (\text{A7})$$

where k_N is defined in Eq. (19) and the notation $G_{nn'}^{\text{FG}}(x, x')$ is used to be distinguished from the true $G_{nn'}^0(x, x')$.

However, this line of reasoning contains a mistake because the contour integral along the infinitely-large semicircle is not negligible for small $|x - x'|$ due to $J_{n-N}(\alpha_0 k) J_{n'-N}(\alpha_0 k)$ in the integrand. This becomes manifest if one represents the Bessel function $J_{n-N}(\alpha_0 k)$ in terms of the Hankel functions as $J_{n-N}(\alpha_0 k) = [H_{n-N}^{(1)}(\alpha_0 k) + H_{n-N}^{(2)}(\alpha_0 k)]/2$ and notes their asymptotic forms

$$H_{n-N}^{(1,2)}(\alpha_0 k) \sim \sqrt{\frac{2}{\pi \alpha_0 k}} \exp \left[\pm i \left(\alpha_0 k - \frac{\pi(n-N)}{2} - \frac{\pi}{4} \right) \right] \quad (\text{A8})$$

in $|\alpha_0 k| \rightarrow \infty$. Especially for $x = x'$, neither of the contour integrals along the semicircles on the upper- and lower-half complex k plane converges due to the coexistence of the terms proportional to $e^{\pm 2i\alpha_0 k}$ in the integrand.

As a result, Eqs. (A6) and (A7) do not satisfy Eq. (A1) at $x = x'$. Namely, Eq. (A1) implies

$$\begin{aligned} & \frac{1}{2} \partial_x G_{nn'}^0(x' + 0, x') - \frac{1}{2} \partial_x G_{nn'}^0(x' - 0, x') \\ & - i\Omega \frac{\alpha_0}{2} \{ [G_{n+1, n'}^0(x' + 0, x') + G_{n-1, n'}^0(x' + 0, x')] - [G_{n+1, n'}^0(x' - 0, x') + G_{n-1, n'}^0(x' - 0, x')] \} = \delta_{nn'}, \end{aligned} \quad (\text{A9})$$

which is obtained by integrating both sides of Eq. (A1) over $x \in [x' - \epsilon, x' + \epsilon]$ and taking the limit of $\epsilon \downarrow 0$. When evaluated for $G_{nn'}^{\text{FG}}(x, x')$ instead of $G_{nn'}^0(x, x')$, the left-

hand side of Eq. (A9) turns out to be

$$\begin{aligned} & \frac{1}{2} \sum_N \left(1 - \frac{(n-N)\Omega}{k_N^2} \right) \\ & \times [1 + (-1)^{n-n'}] J_{n-N}(\alpha_0 k_N) J_{n'-N}(\alpha_0 k_N), \end{aligned} \quad (\text{A10})$$

which is not equal to $\delta_{nn'}$. Thus we have shown $G_{nn'}^{\text{FG}}(x, x') \neq G_{nn'}^0(x, x')$.

We note that the Floquet-Green functions (A6) and (A7) work in the absence of the oscillating electric field. In this case, we do not have the index n , H^0 is just $-\partial_x^2/2$, and the $G^{\text{FG}}(x, x')$ reduces to $-\text{i}e^{\text{i}k_0(x-x')}/k_0$ for $x \geq x'$ and $-\text{i}e^{-\text{i}k_0(x-x')}/k_0$ for $x < x'$. As for Eq. (A9), we do not have the term proportional to Ω , and the condition is satisfied for $G^{\text{FG}}(x, x')$. One can easily show that

Eq. (A5) reduces to

$$\phi^K(0) = \frac{P}{2k_0a} \frac{\sin k_0a}{\cos Ka - \cos k_0a} \phi^K(0), \quad (\text{A11})$$

which gives the dispersion relation (27) for $\phi^K(0) \neq 0$.

At present, the author has not found the proper simplified form of $G_{nn'}^0(x, x')$ yet.

[1] S. Ghimire, A. D. DiChiara, E. Sistrunk, P. Agostini, L. F. DiMauro, and D. A. Reis, *Nature Physics* **7**, 138 (2011).

[2] O. Schubert, M. Hohenleutner, F. Langer, B. Urbanek, C. Lange, U. Huttner, D. Golde, T. Meier, M. Kira, S. W. Koch, and R. Huber, *Nature Photonics* **8**, 119 (2014).

[3] M. Hohenleutner, F. Langer, O. Schubert, M. Knorr, U. Huttner, S. W. Koch, M. Kira, and R. Huber, *Nature* **523**, 572 (2015).

[4] T. T. Luu, M. Garg, S. Y. Kruchinin, A. Moulet, M. T. Hassan, and E. Goulielmakis, *Nature* **521**, 498 (2015).

[5] G. Ndabashimiye, S. Ghimire, M. Wu, D. A. Browne, K. J. Schafer, M. B. Gaarde, and D. A. Reis, *Nature* **534**, 520 (2016).

[6] S. Ghimire, G. Ndabashimiye, A. D. DiChiara, E. Sistrunk, M. I. Stockman, P. Agostini, L. F. DiMauro, and D. A. Reis, *Journal of Physics B: Atomic, Molecular and Optical Physics* **47**, 204030 (2014).

[7] A. McPherson, G. Gibson, H. Jara, U. Johann, T. S. Luk, I. A. McIntyre, K. Boyer, and C. K. Rhodes, *Journal of the Optical Society of America B* **4**, 595 (1987).

[8] M. Ferray, A. L'Huillier, X. F. Li, L. A. Lompre, G. Mainfray, and C. Manus, *Journal of Physics B: Atomic, Molecular and Optical Physics* **21**, L31 (1988).

[9] M. Korbman, S. Yu Kruchinin, and V. S. Yakovlev, *New Journal of Physics* **15**, 013006 (2013).

[10] T. Higuchi, M. I. Stockman, and P. Hommelhoff, *Physical Review Letters* **113**, 213901 (2014).

[11] G. Vampa, C. McDonald, G. Orlando, D. Klug, P. Corkum, and T. Brabec, *Physical Review Letters* **113**, 073901 (2014).

[12] G. Vampa, T. J. Hammond, N. Thiré, B. E. Schmidt, F. Légaré, C. R. McDonald, T. Brabec, and P. B. Corkum, *Nature* **522**, 462 (2015).

[13] D. Golde, T. Meier, and S. W. Koch, *Physical Review B* **77**, 075330 (2008).

[14] C. R. McDonald, G. Vampa, P. B. Corkum, and T. Brabec, *Physical Review A* **92**, 033845 (2015).

[15] P. G. Hawkins, M. Y. Ivanov, and V. S. Yakovlev, *Physical Review A* **91**, 013405 (2015).

[16] M. Wu, S. Ghimire, D. A. Reis, K. J. Schafer, and M. B. Gaarde, *Physical Review A* **91**, 043839 (2015).

[17] T.-Y. Du and X.-B. Bian, *Optics Express* **25**, 151 (2017).

[18] M. Wu, D. A. Browne, K. J. Schafer, and M. B. Gaarde, *Physical Review A* **94**, 063403 (2016).

[19] T. Ikemachi, Y. Shinohara, T. Sato, J. Yumoto, M. Kuwata-Gonokami, and K. L. Ishikawa, *Physical Review A* **95**, 043416 (2017).

[20] G.-R. Jia, X.-H. Huang, and X.-B. Bian, *Optics Express* **25**, 23654 (2017).

[21] T. Ikemachi, Y. Shinohara, T. Sato, J. Yumoto, M. Kuwata-Gonokami, and K. L. Ishikawa, arXiv:1709.08153.

[22] N. Tzoar and J. I. Gersten, *Physical Review B* **12**, 1132 (1975).

[23] F. H. M. Faisal and R. Genieser, *Physics Letters A* **141**, 297 (1989).

[24] F. H. M. Faisal, *Radiation Effects and Defects in Solids* **122-123**, 27 (1991).

[25] F. H. M. Faisal and J. Z. Kamiński, *Physical Review A* **56**, 748 (1997).

[26] A. K. Gupta, O. E. Alon, and N. Moiseyev, *Physical Review B* **68**, 205101 (2003).

[27] O. E. Alon, V. Averbukh, and N. Moiseyev, *Advances in Quantum Chemistry* **47**, 393 (2004).

[28] F. H. M. Faisal, J. Z. Kamiński, and E. Saczuk, *Physical Review A* **72**, 023412 (2005).

[29] R. d. L. Kronig and W. G. Penney, “Quantum Mechanics of Electrons in Crystal Lattices,” (1931).

[30] M. Abramowitz and I. A. Stegun, *Handbook of Mathematical Functions: with Formulas, Graphs, and Mathematical Tables (Dover Books on Mathematics)* (Dover Publications, 1965).